
**MAGNETISM
AND FERROELECTRICITY**

Ab Initio Studies of Dielectric, Piezoelectric, and Elastic Properties of BaTiO₃/SrTiO₃ Ferroelectric Superlattices

A. I. Lebedev

Moscow State University, Moscow, 119991 Russia

e-mail: swan@scon155.phys.msu.su

Received March 2, 2009

Abstract—The phonon spectrum; crystal structure of the polar phase; spontaneous polarization; dielectric constant, piezoelectric, and elastic moduli tensors for free-standing and substrate-supported superlattices $m\text{BaTiO}_3/n\text{SrTiO}_3$ (with $m = n = 1-4$) were calculated within the density functional theory. The simulation of properties of the disordered $\text{Ba}_{0.5}\text{Sr}_{0.5}\text{TiO}_3$ solid solution using two special quasirandom SQS-4 structures and their comparison with the properties of the superlattices revealed a tendency of the $\text{BaTiO}_3\text{—SrTiO}_3$ system to superstructure ordering and showed that the superlattices are thermodynamically quite stable. The ground state of the free-standing superlattice corresponds to the monoclinic polar phase Cm , which transforms to the tetragonal polar phase $P4mm$ under in-plane compressive strain of the superlattice and to the orthorhombic polar phase $Amm2$ under in-plane tensile strain. With a change in the in-plane lattice parameter, in the vicinity of boundaries between neighboring polar phases, some optical and acoustic modes soften and some components of the static dielectric constant, piezoelectric, and elastic moduli tensors diverge critically.

PACS numbers: 64.60.-i, 68.65.Cd, 77.84.Dy, 81.05.Zx

DOI: 10.1134/S1063783409110225

1. INTRODUCTION

Progress in the growth of ferroelectric superlattices (SLs) with a layer thickness controlled with accuracy of one monolayer has opened up new ways for the preparation of multifunctional ferroelectric materials with high values of the spontaneous polarization, Curie temperature, dielectric constant, and its nonlinearity in the electric field. In view of the fact that the properties of ferroelectric superlattices have been poorly studied experimentally to date, their theoretical analysis can enable one to find promising directions of investigation and application of these new materials.

The study of thin epitaxial films of ferroelectrics with a perovskite structure has demonstrated that their properties differ noticeably from those of bulk samples. It has been established that the properties of films are most strongly affected by the mechanical strain produced in them by the substrate. Owing to the strong coupling between the mechanical strain and polarization, these strains have a substantial effect on the ferroelectric phase transition temperature and can lead to the appearance of unusual polar states in thin films [1–4].

Among ferroelectric superlattices, strained $\text{BaTiO}_3/\text{SrTiO}_3$ superlattices have been experimentally investigated most thoroughly to date [5–20]. The first-principles calculations of the properties of these superlattices [18, 19, 21–28] have made it possible to reveal

the main effects responsible for the formation of the polar state in these structures. The specific feature of the superlattices under consideration is that the mechanical strain arising in them due to the difference between the lattice parameters in BaTiO_3 and SrTiO_3 lead to the competition between the polar states in neighboring layers of the superlattice; as a result, the polar phase in the superlattice can appear to be tetragonal, monoclinic, or orthorhombic depending on the mechanical boundary conditions at the interface with the substrate.

However, although the properties of the $\text{BaTiO}_3/\text{SrTiO}_3$ superlattices have been studied in sufficient detail, a number of questions remain open. In particular, first-principles studies of the dielectric properties of these superlattices [23, 24] have revealed only the polar phases $P4mm$ and Cm , whereas the phase $Amm2$, which is characteristic of stretched BaTiO_3 films [2] and $\text{PbTiO}_3/\text{PbZrO}_3$ superlattices [29], has not been found. Fragmentary data on the piezoelectric properties are available only for $\text{PbTiO}_3/\text{PbZrO}_3$ superlattices [30], whereas these data for $\text{BaTiO}_3/\text{SrTiO}_3$ superlattices are absent. Finally, the elastic properties of ferroelectric superlattices and specific features of the behavior of these properties at boundaries between polar phases with different symmetries have not been previously studied at all.

This paper reports on the results of the calculations of the phonon spectrum; crystal structure of the polar

phase; spontaneous polarization; and dielectric constant, piezoelectric, and elastic moduli tensors for free-standing and substrate-supported superlattices $m\text{BaTiO}_3/n\text{SrTiO}_3$ (m/n superlattices) with $m = n = 1-4$. For the 1/1 superlattice as an example, we thoroughly studied the influence of the compression (tension) of the superlattice in the layer plane on the structure and properties of the polar phase; determined the boundaries between the stability regions of the tetragonal, orthorhombic, and monoclinic polar phases; and investigated the specific features of the behavior of the static dielectric constant, piezoelectric, and elastic moduli tensors in the vicinity of these boundaries. Moreover, in the present work, we analyzed the important question regarding the thermodynamic stability of the $\text{BaTiO}_3/\text{SrTiO}_3$ superlattices.

2. CALCULATION TECHNIQUE

The calculations were carried out within the density functional theory with the pseudopotentials and the plane-wave expansion of wave functions as implemented in the ABINIT code [31]. The exchange–correlation interaction was described within the local-density approximation according to the procedure proposed in [32]. As pseudopotentials, we used the optimized separable nonlocal pseudopotentials [33] generated with the OPIUM code to which the local potential was added in order to improve their transferability [34]. The parameters used for constructing the pseudopotentials, the results of their testing, and other details of calculations are described in [35]. In order to increase the accuracy in the determination of the orientation of the polarization vector in the monoclinic phase, the relaxation of atomic positions was performed until the Hellmann–Feynman forces decreased below 5×10^{-6} Ha/Bohr. The phonon spectra and the dielectric, piezoelectric, and elastic properties were calculated in the framework of the density functional theory from the formulas obtained from the perturbation theory. The phonon contribution to the static dielectric constant tensor was calculated from the determined frequencies of phonons and their oscillator strengths [36]. The spontaneous polarization P_s was calculated by the Berry’s phase method [37].

As a rule, epitaxial layers of superlattices are grown on substrates from a material with a cubic structure and the $\langle 100 \rangle$ orientation and the structure of atomic layers reproduces the substrate structure. In this respect, the calculations were carried out for pseudotetragonal lattices, in which the translation vectors in the layer plane have identical length and are directed perpendicular to each other. This means that, in the case of the monoclinic and orthorhombic polar phases, an insignificant (smaller than 0.07°) deviation of angles from 90° was ignored in the calculations. It

was shown that this does not lead to a significant change in the results.

3. RESULTS

3.1. Thermodynamic Properties

For the practical use of the ferroelectric superlattices $\text{BaTiO}_3/\text{SrTiO}_3$, the question of their thermodynamic stability is of crucial importance. This characteristic is determined by the enthalpy of mixing of the superlattice and its relationship to the enthalpy of mixing of the disordered $\text{Ba}_{0.5}\text{Sr}_{0.5}\text{TiO}_3$ solid solution. The most complex part in the first-principles calculation of the enthalpy of mixing is the determination of characteristics of the solid solution, because the direct simulation of lattices with a large number of randomly located atoms makes this problem almost unsolvable.

A fundamentally new approach to the solution of this problem was proposed by Zunger et al. [38], who simulated a disordered solid solution with a special quasirandom structure (SQS), i.e., a short-period superstructure, for which, in the determinate filling of the lattice sites by A and B atoms, the statistical characteristics (the numbers of atomic pairs N_{AA} , N_{BB} , and N_{AB} in several nearest shells) are closest to the corresponding characteristics of an ideal solid solution. This method has been widely used to calculate the electronic structure and physical properties of semiconductor solid solutions and properties of ordering metal alloys. The properties of ferroelectric solid solutions have been rarely studied using this method [39, 40].

The structure of the disordered $\text{Ba}_{0.5}\text{Sr}_{0.5}\text{TiO}_3$ solid solution was simulated with two quasirandom structures SQS-4 with rhombohedral and monoclinic unit cells constructed with the gensqs program of the ATAT code [41]. The translation vectors, order of filling of atomic layers, and pair correlation functions $\bar{\Pi}_{2,m}$ (where m is the number of the shell) describing the deviation of the statistical characteristics of these structures from the ideal solid solution are listed in Table 1. It follows from this table that, in the SQS-4a structure, a noticeable deviation for the values of N_{AA} , N_{BB} , and N_{AB} arises only in the fourth shell, and the SQS-4b structure is characterized by small deviations in the second and fourth shells. The enthalpy of mixing ΔH for the X structures under investigation (superlattices with different periods and SQS-4 structures) was calculated using the formula

$$\Delta H = E_{\text{tot}}(X) - [E_{\text{tot}}(\text{BaTiO}_3) + E_{\text{tot}}(\text{SrTiO}_3)]/2$$

from the values of the total energy E_{tot} (per formula unit) for completely relaxed nonpolar phases. The values of ΔH obtained for these structures are presented in Table 2.

An unexpected result of these calculations was that the value of ΔH for the two shortest period superlat-

Table 1. Translation vectors, order of filling of atomic layers, and statistical characteristics of the SQS-4 structures used for simulating the disordered $\text{Ba}_{0.5}\text{Sr}_{0.5}\text{TiO}_3$ solid solution

Structure	Vectors	Direction	$\bar{\Pi}_{2,1}$	$\bar{\Pi}_{2,2}$	$\bar{\Pi}_{2,3}$	$\bar{\Pi}_{2,4}$
SQS-4a	$[2\bar{1}1], [1\bar{1}2], [1\bar{2}1]$	$AABB\langle 1\bar{1}1\rangle$	0	0	0	-1
SQS-4b	$[210], [\bar{2}10], [001]$	$AABB\langle \bar{1}20\rangle$	0	-1/3	0	1/3

tices appeared to be smaller than the value of ΔH for both realizations of the disordered solid solution. This means that the BaTiO_3 - SrTiO_3 system is prone to *superstructure ordering* of the components. Small values of ΔH for the 1/1 and 2/2 superlattices indicate that the short-period superlattices are thermodynamically quite stable.

Our results differ from the results of the calculations of thermodynamic properties of the BaTiO_3 - SrTiO_3 system by Fuks et al. [42]. The analysis of the calculation technique used in this work showed that, in the calculation of the energies of different superstructures, the authors of [42] did not perform the relaxation of atomic positions and believed that the lattice remains cubic. Therefore, their values of the enthalpy of mixing for the 1/1 superlattice (42 meV per formula unit) include a large excess energy of elastic stresses.

It should be noted that the SQS-4 structures describe rather realistically the local distortions of the solid solution structure. In particular, the predicted interatomic distances in the nonpolar phase are in the ranges 2.738–2.782 Å (SQS-4a) and 2.731–2.782 Å (SQS-4b) for the Sr–O atomic pair and 2.782–2.815 Å (SQS-4a) and 2.776–2.826 Å (SQS-4b) for the Ba–O atomic pair while the interatomic distances in the reference cubic strontium and barium titanates are equal to 2.750 and 2.809 Å. The obtained results are in agreement with the bimodal distribution of bond lengths experimentally revealed for many solid solutions by the EXAFS method.

Table 2. Enthalpies of mixing for several $\text{BaTiO}_3/\text{SrTiO}_3$ superlattices with different layer thicknesses and two SQS-4 structures simulating the disordered $\text{Ba}_{0.5}\text{Sr}_{0.5}\text{TiO}_3$ solid solution

X structure	ΔH , meV
1/1 SL	2.9
2/2 SL	8.9
3/3 SL	11.4
4/4 SL	12.6
SQS-4a	16.8
SQS-4b	11.0

3.2. Ground State of the Strained Superlattice

As was noted in Introduction, the sequentially arranged layers in the $\text{BaTiO}_3/\text{SrTiO}_3$ superlattice produce mutual mechanical stresses in each other; as a result, the SrTiO_3 layers appear to be stretched in the plane and the BaTiO_3 layers turn out to be compressed. If the layers would be isolated, these strains should lead to the appearance of the spontaneous polarization with the vector P_s lying in the layer plane (space group $Amm2$) in the SrTiO_3 layers and to an increase in the polarization directed perpendicularly or at an angle to this plane (space group $P4mm$ or Cm) in the BaTiO_3 layers [1–3]. Since the state with a polarization rapidly varying in space is energetically unfavorable, the question of the orientation of the polarization vector in the ground state of the superlattice needs special consideration. Previous investigations of $\text{PbTiO}_3/\text{PbZrO}_3$ [29] and $\text{BaTiO}_3/\text{SrTiO}_3$ [23, 24] superlattices enable us to expect that the value and orientation of the vector P_s will depend on the substrate-induced strain in the superlattice.

The ground state of the superlattice was searched as follows. For a specified in-plane lattice parameter a_0 (varying in the range from 7.35 to 7.50 Bohr), the equilibrium structure of the nonpolar phase with space group $P4/mmm$ was initially determined by minimizing the Hellmann–Feynman forces. Then, for this structure, the frequencies of the phonon spectrum were calculated at the Γ point. The stable state of the superlattice is characterized by positive values of all frequencies at all points of the Brillouin zone. Therefore, if there were unstable modes (with imaginary mode frequencies) in the phonon spectrum, small perturbations corresponding to the eigenvector of the less stable mode were introduced into the structure and the equilibrium structure of the distorted phase was calculated. The phonon spectrum and equilibrium structure calculations were repeated until the structure with all positive mode frequencies was found.

It should be noted that, in the nonpolar phase of the 1/1 $\text{BaTiO}_3/\text{SrTiO}_3$ superlattice, the ferroelectric mode at the Γ point is the only unstable mode. The well-known instability of the phonon spectrum of SrTiO_3 at the R point of the Brillouin zone disappears in changing over to the superlattice: the phonon energy at the M point of the folded Brillouin zone (into which the R point transforms when doubling the

period along the c axis) in the free-standing 1/1 superlattice is equal to 56 cm^{-1} .

The calculations demonstrated that, for the 1/1 and 2/2 superlattices supported at the SrTiO_3 substrate (the in-plane lattice parameter a_0 is equal to that of cubic strontium titanate, $a_0 = 7.3506 \text{ Bohr}$), the ground state corresponds to the tetragonal polar phase with space group $P4mm$. For the free-standing 1/1 and 2/2 superlattices, the $P4mm$ phase appears to be unstable, undergoes a distortion, and transforms into the monoclinic polar phase Cm . In the 1/1 and 2/2 superlattices stretched in the layer plane, the orthorhombic $Amm2$ phase turns out to be most stable. Therefore, the polar state of the structure can be rather finely controlled by varying the value of a_0 (for example, by growing superlattices on different substrates).

In order to accurately determine the position of the boundaries between the $P4mm$ and Cm phases and between the Cm and $Amm2$ phases, the ground state of the 1/1 superlattice was found for a set of lattice parameters a_0 and the phonon frequencies for each of these structures were calculated at the Γ point. The dependence of the four lowest frequencies on a_0 in phases stable for each lattice parameter is plotted in Fig. 1. It can be seen that, as the boundary between the $P4mm$ and Cm phases is approached from the side of the tetragonal phase, the frequency of the doubly degenerate mode E decreases critically. After the transition to the monoclinic phase, there arise two nondegenerate soft modes A' and A'' in the phonon spectrum, of which the former mode again softens as the boundary between the Cm and $Amm2$ phases is approached. The soft phonon mode on the side of the $Amm2$ phase has a symmetry of B_1 .

By extrapolating (to zero) the dependence of the square of the frequency of the soft ferroelectric modes E in the $P4mm$ phase, A' in the Cm phase, and B_1 in the $Amm2$ phase on a_0 , we determined the lattice parameters corresponding to the boundaries between the polar phases. For the $P4mm$ – Cm transition, the boundary is located at $a_0 = 7.4023 \text{ Bohr}$ in extrapolation from the tetragonal phase and 7.4001 Bohr in extrapolation from the monoclinic phase. For the Cm – $Amm2$ transition, the boundary is located at $a_0 = 7.4489 \text{ Bohr}$ in extrapolation from the orthorhombic phase and 7.4483 Bohr in extrapolation from the mon-

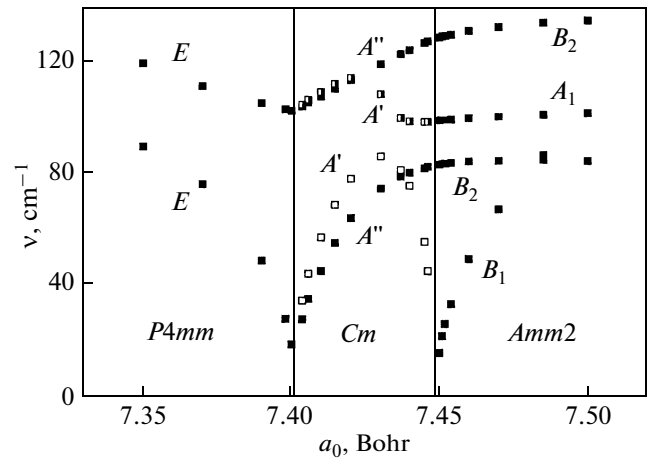


Fig. 1. Dependence of the frequencies of four lowest frequency phonon modes in the polar phase of the 1/1 $\text{BaTiO}_3/\text{SrTiO}_3$ superlattice on the lattice parameter a_0 . The mode symmetry is shown near the curves. Vertical lines indicate the phase stability boundaries.

oclinic phase. A small difference between the values found through the extrapolation from two sides of the transition enables us to believe that both transitions are close to second-order transitions. Since zero strain in the plane of polarized film corresponds to the lattice parameter $a_0 = 7.4462 \text{ Bohr}$, the superlattice strains corresponding to the phase stability boundaries are equal to -0.605 and $+0.032\%$.

3.3. Spontaneous Polarization

As was revealed in Subsection 3.2, the ground state for the 1/1 and 2/2 superlattices supported at the SrTiO_3 substrate corresponds to the tetragonal phase $P4mm$ with the polarization vector directed perpendicularly to the layer plane. The calculations showed that, for supported n/n superlattices, the spontaneous polarization P_s increases monotonically (from 0.277 to 0.307 C/m^2) with an increase in the layer thickness from $n = 1$ to 4 (Table 3). For the free-standing 1/1 and 2/2 superlattices, the ground state corresponds to the monoclinic Cm phase, in which the polarization vector is rotated in the $(\bar{1}10)$ plane from the c axis of the tetragonal nonpolar phase by an angle of 75° for the

Table 3. Spontaneous polarization in the $\text{BaTiO}_3/\text{SrTiO}_3$ superlattices with different layer thicknesses, two QSS-4 structures simulating the disordered $\text{Ba}_{0.5}\text{Sr}_{0.5}\text{TiO}_3$ solid solution, and tetragonal barium titanate

Orientation of \mathbf{P}_s	Structure								
	1/1 SL		2/2 SL		3/3 SL	4/4 SL	QSS-4a	QSS-4b	BaTiO_3
	[xxz]	[001]*	[xxz]	[001]*	[001]*	[001]*	[111]	[001]	[001]
$P_s, \text{C/m}^2$	0.241	0.277	0.252	0.293	0.302	0.307	0.225	0.206	0.259

* Data for the superlattices supported at SrTiO_3 substrate.

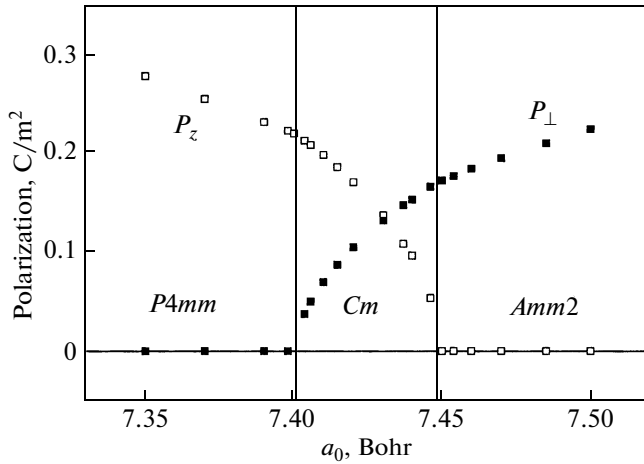


Fig. 2. Decomposition of the polarization vector in the polar phase of the 1/1 BaTiO₃/SrTiO₃ superlattice into the components lying in the layer plane (P_{\perp}) and perpendicular to it (P_z) as a function of the lattice parameter a_0 . Vertical lines indicate the phase stability boundaries.

1/1 superlattice and 63° for the 2/2 superlattice (the values of P_s are given in Table 3). In the 1/1 and 2/2 superlattices stretched in the layer plane, the orthorhombic phase *Amm2*, in which the polarization vector lies in the layer plane and is aligned with the $\langle 110 \rangle$ axis of the tetragonal lattice of the nonpolar phase, appears to be the most stable.

Apart from the data for the superlattices, the calculated values of the spontaneous polarization for the tetragonal BaTiO₃ phase and the disordered Ba_{0.5}Sr_{0.5}TiO₃ solid solution simulated with the SQS-4 structures (see Subsection 3.1) are listed in Table 3. It follows from the table that the values of P_s in all superlattices are larger than those in the solid solution and P_s in superlattices supported at the SrTiO₃ substrate even exceeds the value for tetragonal BaTiO₃. These results agree with the experiment [12].

Figure 2 shows the dependence of the components of polarization, which are parallel and perpendicular to the layer plane, in the polar phase of the 1/1 superlattice on the lattice parameter a_0 . By extrapolating the dependence of P_{\perp}^2 and P_z^2 on a_0 , we find the position of the boundaries for the *P4mm*–*Cm* and *Cm*–*Amm2* transitions: $a_0 = 7.4018$ Bohr and $a_0 = 7.4492$ Bohr, which are very close to the values obtained in Subsection 3.2 from analyzing the dependence of the frequency of the ferroelectric mode on a_0 .

3.4. Dielectric Properties

The dependence of the eigenvalues of the static dielectric constant tensor ϵ_{ij} ($i, j = 1, \dots, 3$) for the 1/1 superlattice on the in-plane lattice parameter a_0 is plotted in Fig. 3. In the tetragonal phase, the eigenvec-

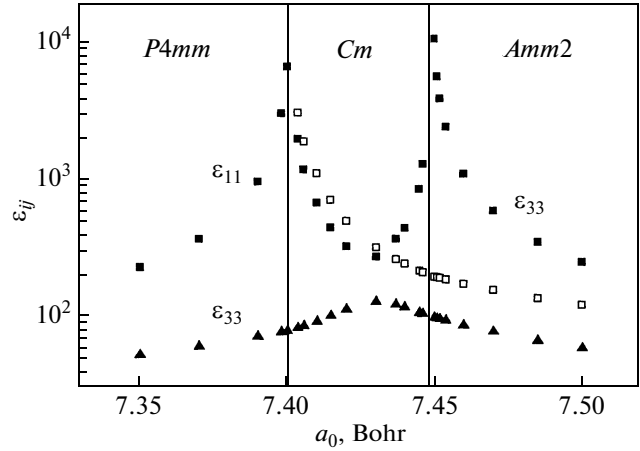


Fig. 3. Dependence of the eigenvalues of the static dielectric constant tensor ϵ_{ij} in the polar phase of the 1/1 BaTiO₃/SrTiO₃ superlattice on the lattice parameter a_0 . Vertical lines indicate the phase stability boundaries. Different symbols represent three different eigenvalues of the dielectric constant tensor.

tors of the tensor ϵ_{ij} are oriented along the crystallographic axes and the eigenvalues ϵ_{11} and ϵ_{22} coincide with each other. Therefore, the dielectric properties of this phase are described by two nonzero independent quantities ϵ_{11} and ϵ_{33} .

In the monoclinic phase, the polarization vector continuously rotates in the $(\bar{1}10)$ plane and none of the eigenvectors of the tensor ϵ_{ij} coincide with the crystallographic axes of the tetragonal lattice of the nonpolar phase. All three eigenvalues are different. In the situation when all nine components of the tensor ϵ_{ij} in the coordinate system of the tetragonal lattice differ from zero, the representation of the eigenvalues of the tensor turns out to be most compact. In the monoclinic phase, the direction of the eigenvector corresponding to the smallest eigenvalue is close but does not coincide with the polarization direction.

In the orthorhombic phase, the eigenvectors of the tensor ϵ_{ij} are oriented along the $\langle 110 \rangle$, $\langle 1\bar{1}0 \rangle$, and $\langle 001 \rangle$ directions of the tetragonal lattice of the nonpolar phase. The vector corresponding to the smallest eigenvalue coincides in direction with the polarization vector, and the vector corresponding to the largest eigenvalue is directed along the $\langle 001 \rangle$ axis.

It follows from Fig. 3 that, with a change in the lattice parameter a_0 , at least one of the eigenvalues of the tensor ϵ_{ij} is characterized by the divergence at the boundaries between the *P4mm* and *Cm* phases and between the *Cm* and *Amm2* phases. As the *P4mm*–*Cm* phase boundary is approached from the tetragonal phase, the components $\epsilon_{11} = \epsilon_{22}$ of this tensor diverge, that is associated with the weakening of the stability of the polarization vector \mathbf{P}_s parallel to $\langle 001 \rangle$ with respect

Table 4. Values of the piezoelectric moduli in the monoclinic phase of the freely suspended superlattice BaTiO₃/SrTiO₃, the tetragonal phase of the same superlattice supported at the SrTiO₃ substrate, and the tetragonal phase of barium titanate

Orientation of \mathbf{P}_s	Structure		
	1/1 SL		BaTiO ₃
	[xxz]	[001]*	[001]
e_{33} , C/m ² (d_{33} , pC/N)	31.9 (460)	7.1 (49)	6.3 (42)
e_{15} , C/m ² (d_{15} , pC/N)	-0.09 (-19)	3.2 (31)	-2.9 (-24)

* Data for the superlattice supported at SrTiO₃ substrate.

to its rotation in the $(\bar{1}10)$ plane. As the boundary between the Cm and $Amm2$ phases is approached from the orthorhombic phase, the component ε_{33} diverges, that is associated with the decrease in the stability of the polarization vector \mathbf{P}_s parallel to $\langle 110 \rangle$ with respect to its rotation in the same plane.

3.5. Piezoelectric Properties

A high sensitivity of the value and direction of the polarization vector in the superlattices to strains enables us to expect that a strong piezoelectric effect appears in them. It is known that anomalously high piezoelectric moduli characteristic of ferroelectrics of the PbZr_{1-x}Ti_xO₃ type in the vicinity of the morphotropic boundary are associated with the easiness of rotation of the polarization vector in the intermediate monoclinic phase under the lattice strain [43, 44]. A similar situation occurs in the monoclinic phase of the BaTiO₃/SrTiO₃ superlattice. As far as we know, up to now, the piezoelectric properties of BaTiO₃/SrTiO₃ ferroelectric superlattices have been studied neither experimentally nor theoretically. The only superlattice for which the piezoelectric properties were calculated was the 1/1 PbTiO₃/PbZrO₃ superlattice, which was used to simulate the properties of the PbTi_{0.5}Zr_{0.5}O₃ solid solution [45].

The results of the calculations of the largest piezoelectric moduli $e_{i\nu}$ ($i = 1, \dots, 3$; $\nu = 1, \dots, 6$) for the tetragonal polar phase of the 1/1 BaTiO₃/SrTiO₃ superlattice supported at the SrTiO₃ substrate and for the monoclinic phase in the same free-standing superlattice are presented in Table 4. It can be seen that the modulus e_{33} in the tetragonal phase differs little from the modulus for tetragonal BaTiO₃. However, for the monoclinic phase, which corresponds to the ground state of the free-standing superlattice, the value of e_{33} appears to be five times larger. A stronger increase in the piezoelectric coefficient d_{35} expressed in pC/N ($d_{i\nu} = \sum_{\mu=1}^6 e_{i\mu} S_{\mu\nu}$) is favored by an increase in the elastic compliance modulus S_{33} by a factor of almost 1.5 upon transition to the monoclinic phase (see in more detail in Subsection 3.6).

Changes in the piezoelectric moduli $e_{i\nu}$ in the polar phase of the 1/1 superlattice with a change in the lattice parameter a_0 are shown in Fig. 4. In the tetragonal phase, according to the symmetry principle, the moduli $e_{31} = e_{32}$, e_{33} and $e_{15} = e_{24}$ (a total of three independent parameters) differ from zero. In the superlattices under investigation, only two of these moduli, i.e., e_{33} and e_{15} , have noticeable values. As the boundary between the $P4mm$ and Cm phases is approached from the tetragonal phase, the value of e_{33} increases monotonically and the modulus e_{15} exhibits a critical behavior and reaches a record high value of 80 C/m² in the vicinity of the boundary.

In the orthorhombic phase in the coordinate system related to the axes of the tetragonal lattice of the nonpolar phase, the moduli $e_{11} = e_{22}$, $e_{12} = e_{21}$, $e_{13} = e_{23}$, $e_{34} = e_{35}$, and $e_{16} = e_{26}$ (a total of five independent parameters) are nonzero. Among them, the moduli e_{11} , e_{12} , e_{34} , and e_{16} are noticeable (Fig. 4). As the boundary between the Cm and $Amm2$ phases is approached, the critical behavior is observed only for

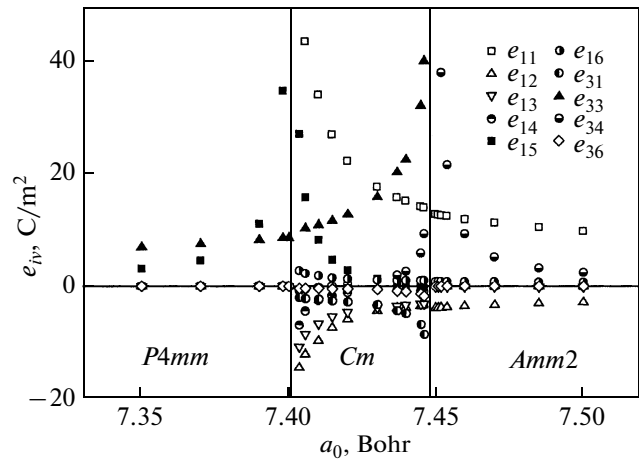


Fig. 4. Dependence of the piezoelectric moduli $e_{i\nu}$ in the polar phase of the 1/1 BaTiO₃/SrTiO₃ superlattice on the lattice parameter a_0 . Vertical lines indicate the phase stability boundaries.

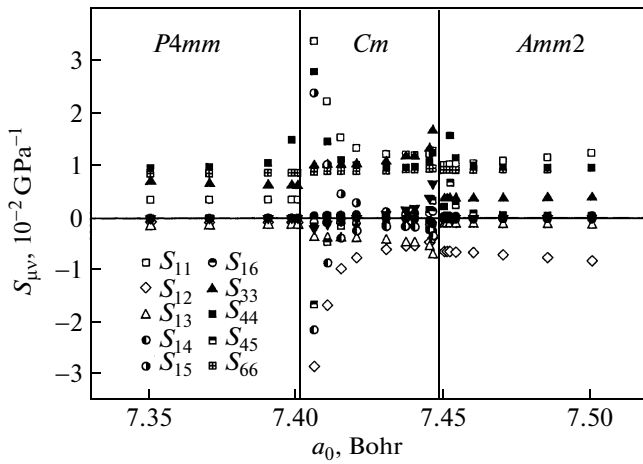


Fig. 5. Dependence of the components of the elastic compliance tensor $S_{\mu\nu}$ in the polar phase of the 1/1 BaTiO₃/SrTiO₃ superlattice on the lattice parameter a_0 . Vertical lines indicate the phase stability boundaries.

the modulus e_{34} , which reaches a value of 192 C/m² in the vicinity of the boundary.

In the monoclinic phase, the behavior of the piezoelectric moduli turns out to be the most complex, because a change in a_0 leads to a continuous rotation of the polarization vector in the $(\bar{1}10)$ plane and all 18 components of the tensor e_{ν} in the coordinate system of the tetragonal lattice of the nonpolar phase differ from zero (the number of independent parameters is equal to ten). It follows from Fig. 4 that, in the monoclinic phase, the critical divergence is observed for the moduli $e_{11} = e_{22}$, $e_{15} = e_{24}$, $e_{12} = e_{21}$, $e_{13} = e_{23}$, $e_{14} = e_{25}$, and $e_{16} = e_{26}$ at the boundary between the *Cm* and *P4mm* phases and the moduli e_{33} , $e_{34} = e_{35}$, $e_{31} = e_{32}$, and e_{36} at the boundary between the *Cm* and *Amm2* phases. It should also be noted that the phase transition is accompanied by a small (by ~10%) stepwise change in the modulus e_{33} (at the *Cm*–*P4mm* boundary) and the moduli e_{11} and e_{12} (at the *Cm*–*Amm2* boundary).

3.6. Elastic Properties

As is known, a ferroelectric phase transition undergoing in a polar crystal is frequently appears to be *ferroelastic*; i.e., it is accompanied by the appearance of soft acoustic modes. This takes place if symmetric second-rank tensor (strain tensor) and polar vector transform according to the same irreducible representation [46]. Since the change in the parameter a_0 leads to transitions between different polar phases in the BaTiO₃/SrTiO₃ superlattices, it is of interest to study the influence of these phase transitions on the elastic properties of superlattices. This is especially important

because the elastic properties of superlattices have not been investigated at all to date.

The elastic compliance tensor $S_{\mu\nu}$ ($\mu, \nu = 1, \dots, 6$) is characterized by six independent and nine nonzero components in the tetragonal *P4mm* phase, nine independent and thirteen nonzero components in the orthorhombic *Amm2* phase (in our coordinate system, the axes of which coincide with those of the tetragonal lattice of the nonpolar phase), and thirteen independent and twenty one nonzero components in the monoclinic *Cm* phase.

The results of the calculations of the components of the elastic compliance tensor for the 1/1 superlattice in the polar state are presented in Fig. 5. It can be seen that, in the vicinity of the boundary between the *P4mm* and *Cm* phases, the components of the tensor $S_{\mu\nu}$ undergo either a stepwise change (moduli $S_{13} = S_{23}$, S_{33} , S_{66} , $S_{16} = S_{26}$, S_{36} , $S_{34} = S_{35}$, $S_{46} = S_{56}$), or a critical divergence on the side of the monoclinic phase (moduli $S_{11} = S_{22}$, S_{12} , $S_{15} = S_{24}$, $S_{14} = S_{25}$, S_{45}). Upon transition to the monoclinic phase, the moduli S_{14} , S_{15} , S_{16} , S_{34} , S_{36} , S_{45} , and S_{46} become nonzero. Upon transition to the orthorhombic phase, the moduli S_{14} , S_{15} , S_{34} , and S_{46} vanish again and the other moduli remain nonzero. At the boundary between the *Cm* and *Amm2* phases, the anomalies of the elastic moduli are less pronounced: the moduli S_{11} , S_{12} , and S_{66} undergo a stepwise change; the moduli S_{13} , S_{14} , S_{15} , S_{16} , S_{33} , S_{34} , S_{36} , and S_{46} are characterized by a weak divergence on the side of the monoclinic phase; and the moduli S_{44} and S_{45} exhibit a weak divergence on both sides of the boundary.

The critical divergence of the modulus S_{44} at both boundaries *P4mm*–*Cm* and *Cm*–*Amm2* suggests that the phase transitions occurring under continuous tension of the superlattice in the layer plane are ferroelastic.

4. DISCUSSION OF THE RESULTS

The results obtained in this work, which describe the influence of strains on the crystal structure of the BaTiO₃/SrTiO₃ superlattice in its ground state, are not in complete agreement with the results of the calculations performed in [18, 22–24]. These results agree with each other in that the ground state of the free-standing 1/1 BaTiO₃/SrTiO₃ superlattice corresponds to the monoclinic *Cm* phase, the in-plane compression leads to the transition between the *Cm* and *P4mm* phases, and the dielectric constant at the phase boundary exhibits a divergence. However, unlike our results, the authors of [23, 24] did not succeed in revealing the transition between the monoclinic and orthorhombic polar phases, even though they observed an almost complete rotation of the polarization vector

to the $\langle 110 \rangle$ direction. The absence of this transition was indicated in [24] by the fact that the frequencies of all optical modes in the Cm phase remained real and increased under tension of the superlattice. We believe that our results are more correct because they are in agreement with the results obtained for $BaTiO_3$ [2] and $SrTiO_3$ [47] thin strained films, the data of the recent calculations for the 2/2 $BaTiO_3/SrTiO_3$ superlattice [25], and the results of the studies of one more $PbTiO_3/PbZrO_3$ superlattice [29]. In all these works the phase sequence $P4mm-Cm-Amm2$ was observed under tension of superlattices in the layer plane.

Small differences between our data for the $P4mm-Cm$ transition and the data obtained in [23] lie in the value of the minimum spontaneous polarization, which appeared to be 75% higher in our work, and in a somewhat different position of the boundary between the tetragonal and monoclinic phases.

Unfortunately, an insufficient amount of data on the dielectric properties of $BaTiO_3/SrTiO_3$ superlattices in [24] does not enable us to thoroughly compare them with our results. However, a comparison of our data with the results of the calculations of the dielectric properties of $PbTiO_3/PbZrO_3$ superlattices [29] demonstrates that all eigenvalues of the dielectric constant tensor in the monoclinic phase of the $BaTiO_3/SrTiO_3$ superlattices turn out to be higher; i.e., these superlattices can be more promising for practical applications.

Before preceding to the discussion of the piezoelectric properties of the strained $BaTiO_3/SrTiO_3$ superlattices, it should be noted that the situations in which characteristics of superlattices, such as e_{iv} and $S_{\mu\nu}$, exhibit a divergence can be of greatest practical importance. As was shown in Subsections 3.5 and 3.6, these situations arise in the vicinity of the boundaries between the phases. The calculations demonstrate that, in the vicinity of the $P4mm-Cm$ boundary, the piezoelectric coefficient d_{11} , which reached a value of 2300 pC/N, is the largest in the monoclinic phase, and the coefficient d_{15} , which reached a value of 6200 pC/N, is the largest in the tetragonal phase. In the vicinity of the $Cm-Amm2$ boundary, the coefficient d_{33} , which reached a value of 9200 pC/N, is the largest in the monoclinic phase, and the coefficient d_{34} (10500 pC/N) is the largest in the orthorhombic phase. For comparison, we note that the record value of the piezoelectric coefficient obtained for crystals in the $Pb(Zn_{1/3}Nb_{2/3})O_3-PbTiO_3$ system is 2500 pC/N [48]. An anomalous increase in the calculated coefficients d_{15} and d_{33} to values of ~ 8500 pC/N in the vicinity of the $P4mm-Cm$ boundary was also predicted for isotropically compressed $PbTiO_3$ [49].

Now, we discuss the elastic properties of the superlattices and the results indicating the appearance of ferroelastic phase transitions. According to [46], the phase transition $4mm \rightarrow m$ in crystals with space

group $P4mm$ should exhibit ferroelastic properties. Upon this phase transition, lattice distortions are characterized by one or both nonzero strain tensor components u_4 and u_5 , and a soft transverse acoustic phonon with the wave vector directed along the polar axis should appear in the phonon spectrum. The direct calculations of the frequencies of acoustic modes in the tetragonal phase at the point of the Brillouin zone with the reduced wave vector $\mathbf{q} = (0, 0, 0.05)$ confirmed this fact: as the $P4mm-Cm$ boundary is approached, the frequency of the doubly degenerate transverse acoustic phonon with symmetry Λ_5 decreases by a factor of five. The softening of this phonon is directly associated with the divergence of the elastic compliance moduli $S_{44} = S_{55}$.

The ferroelastic phase transition should also occur at the boundary between the Cm and $Amm2$ phases. According to [46], the transition $mm2 \rightarrow m$ should be accompanied by the lattice distortion described by one nonzero of three strain tensor components u_4 , u_5 , and u_6 . In the chosen coordinate system with the orientation of the polar axis along the $\langle 110 \rangle$ direction (unusual for the orthorhombic lattice), the softening of the transverse acoustic phonon with a wave vector directed along this axis should appear. The direct calculations of the frequencies of acoustic modes in the orthorhombic phase at the point of the Brillouin zone with the reduced wave vector $\mathbf{q} = (0.035, 0.035, 0)$ confirmed this fact. Most likely, the specific orientation of the polar axis is responsible for the fact that the anomalies in the elastic compliance tensor at the ferroelastic phase transition $Cm \rightarrow Amm2$ are rather weakly pronounced. For the same reason, some components of the elastic compliance tensor appear to be related to each other: for example, the moduli S_{44} and S_{45} that exhibit the divergence in the orthorhombic phase satisfy the expression $S_{44} - S_{45} \approx \text{const}$ in this phase.

An intriguing feature revealed in our work is that the character of atomic displacements in unstable ferroelastic modes in the 1/1 and 2/2 superlattices in the $P4/mmm$ phase are quantitatively different: all metal atoms in the 1/1 superlattice move in antiphase with oxygen atoms for all three polarizations of vibrations, whereas, in the 2/2 superlattice, this holds true only for the A_{2u} mode. For the E_u mode, the amplitude of the displacement of different titanium atoms differs by a factor of approximately three and both Ba atoms vibrate in phase with O atoms and antiphase with Ti and Sr atoms.

5. CONCLUSIONS

Thus, in the present work, the properties of the $mBaTiO_3/nSrTiO_3$ superlattices (with $m = n = 1, \dots, 4$) were calculated within the density functional theory. A comparison of the properties of the superlattices with the properties of the disordered $Ba_{0.5}Sr_{0.5}TiO_3$ solid

solution simulated with the special quasirandom structures SQS-4 showed that the BaTiO₃-SrTiO₃ system has a tendency to superstructure ordering of the components and that the superlattices themselves are thermodynamically quite stable. The ground state of the free-standing superlattice corresponds to the monoclinic polar phase *Cm*, which transforms to the tetragonal polar phase *P4mm* under the in-plane compression of the superlattice and to the orthorhombic polar phase *Amm2* under the in-plane tension of the superlattice. All components of the dielectric constant (ϵ_{ij}), piezoelectric moduli (e_{iv}), and elastic moduli ($S_{\mu\nu}$) tensors were calculated as a function of the in-plane strain of the superlattices. It was demonstrated that the dielectric constant in the monoclinic phase of the superlattices is noticeably higher than that in the same phase of the PbTiO₃/PbZrO₃ superlattices. The critical behavior of the components of the tensors ϵ_{ij} , e_{iv} , and $S_{\mu\nu}$ was studied in the vicinity of the boundaries between different polar phases, and it was shown that the transitions between these phases are ferroelastic. It was demonstrated that uniquely high piezoelectric parameters can be achieved by finely controlling the superlattice strain.

ACKNOWLEDGMENTS

This work was supported by the Russian Foundation for Basic Research (project no. 08-02-01436).

REFERENCES

- N. A. Pertsev, A. G. Zembilgotov, and A. K. Tagantsev, Phys. Rev. Lett. **80**, 1988 (1998).
- O. Diéguez, S. Tinte, A. Antons, C. Bungaro, J. B. Neaton, K. M. Rabe, and D. Vanderbilt, Phys. Rev. B: Condens. Matter **69**, 212101 (2004).
- J. H. Haeni, P. Irvin, W. Chang, R. Uecker, P. Reiche, Y. L. Li, S. Choudhury, W. Tian, M. E. Hawley, B. Craigo, A. K. Tagantsev, X. Q. Pan, S. K. Streiffner, L. Q. Chen, S. W. Kirchoefer, J. Levy, and D. G. Schlom, Nature (London) **430**, 758 (2004).
- M. Dawber, K. M. Rabe, and J. F. Scott, Rev. Mod. Phys. **77**, 1083 (2005).
- K. Iijima, T. Terashima, Y. Bando, K. Kamigaki, and H. Terauchi, J. Appl. Phys. **72**, 2840 (1992).
- E. Wiener-Avnear, Appl. Phys. Lett. **65**, 1784 (1994).
- H. Tabata, H. Tanaka, and T. Kawai, Appl. Phys. Lett. **65**, 1970 (1994).
- H. Tabata and T. Kawai, Appl. Phys. Lett. **70**, 321 (1997).
- T. Zhao, Z.-H. Chen, F. Chen, W.-S. Shi, H.-B. Lu, and G.-Z. Yang, Phys. Rev. B: Condens. Matter **60**, 1697 (1999).
- O. Nakagawara, T. Shimuta, T. Makino, S. Arai, H. Tabata, and T. Kawai, Appl. Phys. Lett. **77**, 3257 (2000).
- T. Tsurumi, T. Ichikawa, T. Harigai, H. Kakemoto, and S. Wada, J. Appl. Phys. **91**, 2284 (2002).
- T. Shimuta, O. Nakagawara, T. Makino, S. Arai, H. Tabata, and T. Kawai, J. Appl. Phys. **91**, 2290 (2002).
- J. Kim, Y. Kim, Y. S. Kim, J. Lee, L. Kim, and D. Jung, Appl. Phys. Lett. **80**, 3581 (2002).
- S. Rios, A. Ruediger, A. Q. Jiang, J. F. Scott, H. Lu, and Z. Chen, J. Phys.: Condens. Matter **15**, L305 (2003).
- A. Q. Jiang, J. F. Scott, H. Lu, and Z. Chen, J. Appl. Phys. **93**, 1180 (2003).
- F. Q. Tong, W. X. Yu, F. Liu, Y. Zuo, and X. Ge, Mater. Sci. Eng., B **98**, 6 (2003).
- T. Harigai, D. Tanaka, H. Kakemoto, S. Wada, and T. Tsurumi, J. Appl. Phys. **94**, 7923 (2003).
- J. Lee, L. Kim, J. Kim, D. Jung, and U. V. Waghmare, J. Appl. Phys. **100**, 051613 (2006).
- W. Tian, J. C. Jiang, X. Q. Pan, J. H. Haeni, Y. L. Li, L. Q. Chen, D. G. Schlom, J. B. Neaton, K. M. Rabe, and Q. X. Jia, Appl. Phys. Lett. **89**, 092905 (2006).
- B. R. Kim, T.-U. Kim, W.-J. Lee, J. H. Moon, B.-T. Lee, H. S. Kim, and J. H. Kim, Thin Solid Films **515**, 6438 (2007).
- J. B. Neaton and K. M. Rabe, Appl. Phys. Lett. **82**, 1586 (2003).
- K. Johnston, X. Huang, J. B. Neaton, and K. M. Rabe, Phys. Rev. B: Condens. Matter **71**, 100103 (2005).
- L. Kim, J. Kim, D. Jung, J. Lee, and U. V. Waghmare, Appl. Phys. Lett. **87**, 052903 (2005).
- L. Kim, J. Kim, U. V. Waghmare, D. Jung, and J. Lee, Phys. Rev. B: Condens. Matter **72**, 214121 (2005).
- S. Lisenkov and L. Bellaiche, Phys. Rev. B: Condens. Matter **76**, 020102 (2007).
- J. H. Lee, U. V. Waghmare, and J. Yu, J. Appl. Phys. **103**, 124106 (2008).
- Z. Y. Zhu, H. Y. Zhang, M. Tan, X. H. Zhang, and J. C. Han, J. Phys. D: Appl. Phys. **41**, 215408 (2008).
- S. Lisenkov, I. Ponomareva, and L. Bellaiche, Phys. Rev. B: Condens. Matter **79**, 024101 (2009).
- C. Bungaro and K. M. Rabe, Phys. Rev. B: Condens. Matter **69**, 184101 (2004).
- G. Sághi-Szabó, R. E. Cohen, and H. Krakauer, Phys. Rev. B: Condens. Matter **59**, 12771 (1999).
- X. Gonze, J.-M. Beuken, R. Caracas, F. Detraux, M. Fuchs, G.-M. Rignanese, L. Sindic, M. Verstraete, G. Zerath, F. Jollet, M. Torrent, A. Roy, M. Mikami, Ph. Ghosez, J.-Y. Raty, and D. C. Allan, Comput. Mater. Sci. **25**, 478 (2002).
- J. P. Perdew and A. Zunger, Phys. Rev. B: Condens. Matter **23**, 5048 (1981).
- A. M. Rappe, K. M. Rabe, E. Kaxiras, and J. D. Joannopoulos, Phys. Rev. B: Condens. Matter **41**, 1227 (1990).
- N. J. Ramer and A. M. Rappe, Phys. Rev. B: Condens. Matter **59**, 12471 (1999).
- A. I. Lebedev, Fiz. Tverd. Tela (St. Petersburg) **51** (2), 341 (2009) [Phys. Solid State **51** (2), 362 (2009)].
- G.-M. Rignanese, X. Gonze, and A. Pasquarello, Phys. Rev. B: Condens. Matter **63**, 104305 (2001).
- R. D. King-Smith and D. Vanderbilt, Phys. Rev. B: Condens. Matter **47**, 1651 (1993).

38. A. Zunger, S.-H. Wei, L. G. Ferreira, and J. E. Bernard, *Phys. Rev. Lett.* **65**, 353 (1990).
39. B. P. Burton and E. Cockayne, *Ferroelectrics* **270**, 173 (2002).
40. S. A. Prosandeev, E. Cockayne, B. P. Burton, S. Kamba, J. Petzelt, Yu. Yuzyuk, R. S. Katiyar, and S. B. Vakhrushev, *Phys. Rev. B: Condens. Matter* **70**, 134110 (2004).
41. A. van de Walle and G. Ceder, *J. Phase Equilib.* **23**, 348 (2002).
42. D. Fuks, S. Dorfman, S. Piskunov, and E. A. Kotomin, *Phys. Rev. B: Condens. Matter* **71**, 014111 (2005).
43. H. Fu and R. E. Cohen, *Nature (London)* **403**, 281 (2000).
44. R. Guo, L. E. Cross, S.-E. Park, B. Noheda, D. E. Cox, and G. Shirane, *Phys. Rev. Lett.* **84**, 5423 (2000).
45. Z. Wu and H. Krakauer, *Phys. Rev. B: Condens. Matter* **68**, 014112 (2003).
46. R. Blinc and B. Žekš, *Soft Modes in Ferroelectrics and Antiferroelectrics* (North-Holland, Amsterdam, 1974; Mir, Moscow, 1975).
47. A. Antons, J. B. Neaton, K. M. Rabe, and D. Vanderbilt, *Phys. Rev. B: Condens. Matter* **71**, 024102 (2005).
48. S.-E. Park and T. R. ShROUT, *J. Appl. Phys.* **82**, 1804 (1997).
49. Z. Wu and R. E. Cohen, *Phys. Rev. Lett.* **95**, 037601 (2005).